

# First Principles Study of the Structure and Chemistry of Mg-Based Hydrotalcite-Like Anionic Clays

Andrea Trave,<sup>\*,†,‡</sup> Annabella Selloni,<sup>‡</sup> Annick Goursot,<sup>†,§</sup> Didier Tichit,<sup>§</sup> and Jacques Weber<sup>†</sup>

Department of Physical Chemistry, University of Geneva, CH-1211 Geneva, Switzerland,

Department of Chemistry, Princeton University, Princeton, New Jersey 08544, and

Ecole de Chimie, UMR 5618 CNRS, F-34296 Montpellier, Cedex5, France

Received: June 19, 2002; In Final Form: September 19, 2002

We use variable-cell first principles molecular dynamics as an optimization tool to investigate the structural and electronic properties of Mg-based anhydrous hydrotalcite-like compounds. The formation energy as a function of the ratio  $R$  between di- and trivalent cations shows a minimum at  $R \sim 3$ , in good agreement with experimental stability ranges for these materials. At the same value  $R \sim 3$ , a maximum is found in the calculated interlayer distance, suggesting a correlation between energetic stability and structure. The energies and character of the electronic states of hydrotalcites containing different interlayer anions and trivalent cations have been compared. The nature of the anions is found to have a major influence on the electronic properties. In particular,  $\text{OH}^-$  anions, rather than, e.g.,  $\text{Cl}^-$ , lead to a significantly smaller HOMO–LUMO gap, with a LUMO spatially more localized in the interlayer region. These features are related to the observed differences in the catalytic properties of hydrotalcites containing  $\text{OH}^-$  vs  $\text{Cl}^-$  anions.

## I. Introduction

Hydrotalcite is, in its natural form, a hydroxycarbonate of magnesium and aluminum, belonging to the class of anionic clays, with the formula  $[\text{Mg}_6\text{Al}_2(\text{OH})_{16}]^{2+} \cdot \text{CO}_3^{2-} \cdot 4\text{H}_2\text{O}$ , and a layered structure. Its name designates a whole class of natural or synthetic *hydrotalcite-like compounds* (HTLcs), with generic formula



where  $\text{M}^{\text{II}}$  is a divalent metal (Mg, Ni, Zn, Cu, ...),  $\text{M}^{\text{III}}$  a trivalent metal (Al, Ga, Cr, Fe,...), and  $\text{A}^{n-}$  an  $n$ -valent anion ( $\text{CO}_3^{2-}$ ,  $\text{OH}^-$ ,  $\text{Cl}^-$ ,  $\text{SO}_4^{2-}$ , ...) <sup>1</sup>. The  $\text{M}^{\text{II}}/\text{M}^{\text{III}}$  ratio  $R = (1 - x)/x$  is usually in the range  $1.5 \lesssim R \lesssim 4$ .<sup>2</sup>

HTLcs are gaining considerable interest in several technological fields, particularly for base-catalyzed reactions. Their properties and applications have been the subject of detailed reviews,<sup>1–3</sup> and many publications have provided examples of their practical uses. However, many aspects of their behavior which depend on the chemical composition still require clarification, for example, changes of the basic activity. Indeed, a larger basicity is found when Ga is used instead of Al,<sup>4,5</sup> and/or when OH, rather than Cl, is used as a counterion.<sup>6,7</sup> As these findings have a potentially strong impact on industrial applications, an understanding of the connection between HTLc's chemical activity and composition is highly desirable.

Molecular dynamics simulations based on first principles interatomic potentials<sup>8,9</sup> have proven to be a powerful tool for obtaining microscopic insight into the atomic and electronic properties of materials, and their evolution with respect to chemical changes. This approach has already been extensively

applied to a large variety of oxide materials, but no work on HTLcs is available yet, except for a recent study of the related  $\text{Mg}(\text{OH})_2$  system.<sup>10</sup> In this paper, we shall use constant-volume<sup>8</sup> and variable-cell<sup>11–13</sup> ab initio MD as an optimization tool to study the correlations between chemical composition, microscopic atomic structure, and electronic properties in a series of *anhydrous* HTLcs with different compositions. After brief reviews of some experimental facts (section II) and of the theoretical approach (section III), in section IV we study the structural parameters and the formation energy of HTLcs based on Mg and Al, with Cl anions, as functions of the Al/Mg ratio  $R$ . Finally, in section V, the dependence of structural and electronic properties on chemical composition is examined by studying three different HTLcs all having the same value of  $R$ , i.e.,  $[\text{Mg}_3\text{Al}(\text{OH})_8] \cdot \text{Cl}$ ,  $[\text{Mg}_3\text{Al}(\text{OH})_8] \cdot \text{OH}$ , and  $[\text{Mg}_3\text{Ga}(\text{OH})_8] \cdot \text{OH}$ . In particular, we compare  $[\text{Mg}_3\text{Al}(\text{OH})_8] \cdot \text{Cl}$  and  $[\text{Mg}_3\text{Al}(\text{OH})_8] \cdot \text{OH}$ , which correspond to the same substrate but contain anions with different basicity, on one hand, and  $[\text{Mg}_3\text{Ga}(\text{OH})_8] \cdot \text{OH}$  and  $[\text{Mg}_3\text{Al}(\text{OH})_8] \cdot \text{OH}$ , which have identical anions but different substrates, on the other.

## II. Structure and Properties of Hydrotalcite-Like Compounds: A Summary

HTLcs are structurally similar to brucite  $\text{Mg}(\text{OH})_2$ : layers of edge-sharing octahedral units, formed by a divalent cation (partially substituted by a trivalent one) coordinated to six hydroxyl groups, are stacked one on top of the other, and intercalated by interlayer regions containing water molecules and charge-balancing anions. Because of their characteristic structure, this class of materials goes also under the name of *layered double hydroxides* (LDH). The structures of several HTLcs have been first investigated by Allmann<sup>14,15</sup> and further characterized in more recent works.<sup>16–18</sup>

HTLcs can be characterized in terms of various parameters related to their chemical composition and microscopic structure. We already mentioned the important  $\text{M}^{\text{II}}/\text{M}^{\text{III}}$  ratio  $R$ , which is directly connected to the stability of the material. Depending

\* Corresponding author. Current address: Department of Physics, University of California, Berkeley, CA 94720-7300. E-mail: atrave@civet.berkeley.edu.

<sup>†</sup> University of Geneva.

<sup>‡</sup> Princeton University.

<sup>§</sup> UMR 5618 CNRS.

on the chemical composition, HTlcs can be found in nature or synthesized within a certain range of values for  $R$ , whereas outside these limits there is segregation of pure  $M^{II}$  or  $M^{III}$  metal hydroxide aggregates. Pure [Mg,Al]-HTlc was theoretically predicted to exist only in the range  $2 \lesssim R \lesssim 3.5$ ,<sup>19</sup> but these limits have been successfully pushed down to  $R \sim 1.3$ <sup>20</sup> and up to  $R \sim 5$ .<sup>21</sup> [Mg,Ga]-HTlc has a larger range of stability  $1.8 \lesssim R \lesssim 12.9$ , due to the smaller difference of the ionic radii for the Mg–Ga pair with respect to Mg–Al.<sup>22</sup>

The number of anions depends on  $R$ , as it exactly counterbalances the layer charge introduced by the trivalent atoms. In the same way, the concentration of water in the formula is directly related to the number of anions, and consequently to  $R$ , as water molecules usually fill the interlayer space left unoccupied among the anions.<sup>23</sup> However, the hydration can be strongly reduced by acting on the synthesis conditions<sup>19</sup> or with a subsequent calcination.<sup>2</sup>

Another defining characteristic of HTlcs is the stacking sequence of the brucite-like layers. Looking at a single layer from the top, cations and oxygen atoms are hexagonally distributed, occupying respectively sites indicated as A (cation), B (oxygen above the midlayer plane), and C (oxygen under it), whereas the O–H bonds of the hydroxyl groups are vertically oriented and aligned with the OH groups of the other layers. A class of HTlcs, represented by natural hydrotalcite, has a 3R rhombohedral unit cell of parameters  $a$  (characterizing the distances within a layer) and  $c = 3c'$  (where  $c'$  is the basal distance between two layers), consisting of three layers with the OH groups aligned in the sequence BC–CA–AB–BC–.... A second form of HTlcs, represented by manasseite, has a 2H hexagonal cell of parameters  $a$  and  $c = 2c'$ , containing two layers stacked as BC–CB–BC–....<sup>24</sup> In nature, the two forms can be often found intergrown. Brucite is yet different, with a 1H single-layer stacking, BC–BC–..., and a different disposition of the hydroxyl groups across the interlayer space, where each OH is surrounded by three OH groups in the facing layer. This stacking sequence has been reported also for some HTlcs.<sup>25</sup>

Anionic clays are much less frequent in nature than cationic ones. While for a long time their interest was just mineralogical, in recent years the possibility of technological applications of HTlcs, as such or as precursors to other active materials, has become apparent. The presence of highly mobile anions and the Brønsted basicity of the layer surfaces have great importance for direct catalysis or catalyst support, and other uses include ion exchange, anion adsorption, and molecular stabilization. The easy control on the composition of synthetic HTlcs and the possibility to increase the active surface area and the interlayer volume with appropriate choices of the intercalated anions allow to finely tune the properties of the material to meet the desired requirements.

### III. Theoretical/Computational Approach

The variable-cell first-principles molecular dynamics (FPMD) combines the standard (constant-volume) FPMD approach,<sup>8,9,26</sup> where interatomic forces are explicitly calculated from the electronic ground state obtained from density functional theory (DFT),<sup>27</sup> with the method introduced by Parrinello and Rahman<sup>11</sup> to perform classical simulations with constant pressure conditions. In standard FPMD the shape and size of the simulation cell is fixed at the start and cannot be changed during the calculations (fixed-cell MD). Parrinello and Rahman,<sup>11</sup> extending a method originally proposed by Andersen<sup>28</sup> for constant-pressure simulations, introduced a scheme, in which the simulation cell could follow not only isotropic volume

**TABLE 1: Calculated Geometrical Parameters for Brucite  $Mg(OH)_2$ , Compared to the Experimental Values<sup>34</sup>**

	simulation	experiment <sup>34</sup>
molar vol (cm <sup>3</sup> /mol)	22.605	24.524
$a$ (Å)	3.110	3.124
$c$ (Å)	4.476	4.766
MgO (Å)	2.067	2.102
layer thickness (Å)	2.043	2.112

changes but also anisotropic shape distortions. This is done via a Lagrangian for an extended system, including the atomic degrees of freedom and the matrix formed by the three primitive Bravais vectors defining the cell.

The first successful application of a constant-pressure simulation method with a first principles approach was made by Focher et al.,<sup>12,13</sup> and since then this approach has proven extremely useful for the study of phase transformations and material properties under pressure.<sup>29</sup> With respect to refs 12 and 13, the implementation used in this work includes new features, such as the efficient treatment of ultrasoft pseudopotentials<sup>30</sup> introduced in ref 31. In this work, however, we use the variable-cell FPMD only as an optimization tool for a complex structure with many atoms per unit cell. We simultaneously relax both the atomic coordinates and the three unit cell vectors until they reach their zero-pressure optimum value. Friction forces have been applied to all degrees of freedom to allow for a dynamical minimization of the total energy. A run would typically be continued until the total kinetic energy associated with the atomic and cell degrees of freedom would be less than  $10^{-5}$  au.

As in standard FPMD, we expand the electronic wave functions in plane waves. The approach of Bernasconi et al.<sup>13</sup> was followed to maintain a constant energy cutoff in variable cell simulations. We describe electron–ion interactions in terms of pseudopotentials. In particular, norm-conserving<sup>32</sup> pseudopotentials have been used for all atomic species but oxygen, for which an ultrasoft<sup>30</sup> potential was employed.

Unless otherwise specified, we use the generalized gradient approximation (GGA)<sup>33</sup> for the exchange–correlation energy and potential, and an energy cutoff of 25 Ry for the plane wave expansion. In most calculations, the simulation cell contains 16 formula units, with two layers of 8 octahedra each, and a total number of 83–86 atoms. This choice does not allow the simulation of structures with a 3-fold 3R stacking, the most common in hydrotalcite-like materials, which would require very large and cumbersome calculations. However, because the local structure of the layers should not be significantly affected by this choice, the comparison of our results with the experimental data is justified.

As a preliminary test, we applied the variable cell FPMD to calculate the equilibrium structure of brucite  $Mg(OH)_2$ , and compared it to experimental data<sup>34</sup> (see Table 1). The agreement is good for what concerns the intralayer geometries, whereas the calculated interlayer distance is underestimated by  $\sim 6\%$ . This may be related to the fact that the weak interlayer forces of brucite are not well described in DFT. This problem should be less serious in HTlcs where rather strong electrostatic interlayer interactions are present.

### IV. Results: Structural Properties of [Mg,Al][Cl]-HTlcs

In the following we study anhydrous hydrotalcite-like samples, containing Mg and Al as the divalent and trivalent cations respectively, and Cl as the counterion. In subsection IVA the

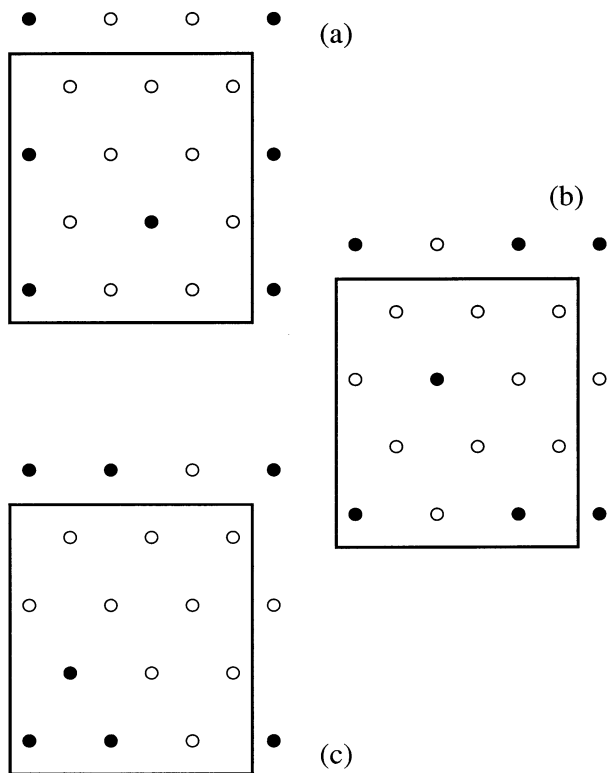


**Figure 1.** Schematic top view of the layers in the HTlc samples of the first simulation series. Empty and solid circles are respectively Mg and Al atoms. The contour of the simulation cell is indicated.

arrangement of Al cations is optimized at fixed stoichiometry. The dependence on the Mg/Al ratio  $R$  is analyzed in subsection IVB.

**A. Ordering of Trivalent Cations.** We examined the effect of variable cation ordering in a sample of fixed composition  $R = 3$ , i.e.,  $[\text{Mg}_3\text{Al}(\text{OH})_8]\cdot\text{Cl}$ . To expedite the calculations, the volume of the simulation cell was kept fixed, and the experimental cell parameters were used ( $a = 3.046 \text{ \AA}$ ;  $c' = 7.591 \text{ \AA}$ <sup>18</sup>). The local density approximation (LDA)<sup>35</sup> was used and the energy cutoff in the plane wave expansion was 16 Ry. The simulation cell contained 24 formula units, with two layers of 12 octahedra each, stacked in a 2H sequence (BC–CB–BC–...), and a total number of 126 atoms.

In Figure 1 the studied configurations are sketched. In configuration (a), the distribution of trivalent Al cations is such that their distances are maximized and no pairs of adjacent Al's are found. Moreover, the Al cations are vertically aligned in the two layers. In configuration (b), each layer of the simulation cell has a pair of adjacent Al atoms, whereas in configuration (c) the Al's form small clusters of nearest neighbor atoms. After relaxation, we find that the total energies of configurations (b) and (c) are  $7.3 \times 10^{-2}$  and  $12.2 \times 10^{-2} \text{ eV/Al}$  higher than configuration (a), respectively. Finally, we examined a fourth configuration, (d), with the same intralayer Al ordering than (a), but with a relative horizontal shift of the layers that eliminates the vertical alignment of the Al's. In this way, the Al's are stacked in a rhombohedral sequence, instead of hexagonal. The calculated energy difference with respect to (a) is still positive,  $5.2 \times 10^{-2} \text{ eV/Al}$ .

These results show that a homogeneous ordering of trivalent cations, minimizing cation–cation repulsive interactions, is energetically favored with respect to configurations with adjacent Al atoms, in agreement with the cation avoidance rule.<sup>36</sup> This behavior has been experimentally observed, particularly

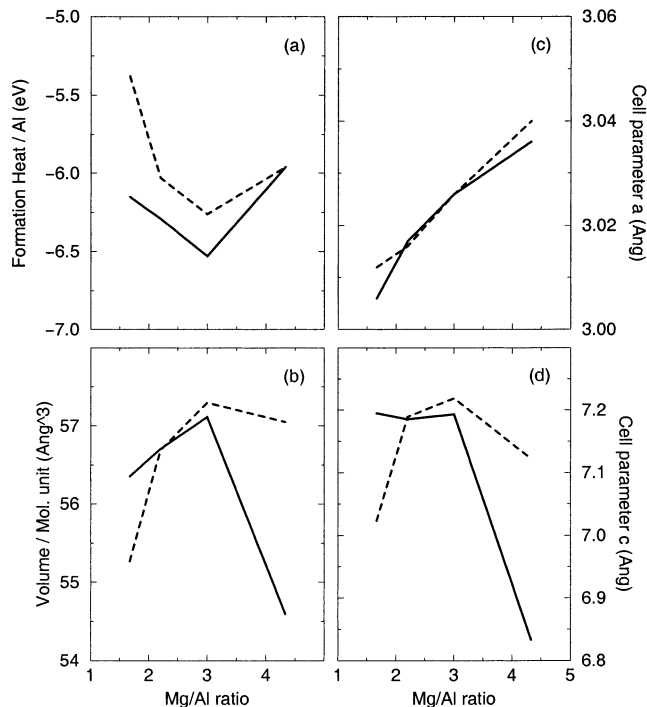


**Figure 2.** Energetic and geometrical parameters for hydrotalcite with variable Mg/Al ratio and stacking 2H (solid line) and 1H (dashed line): (a) formation heat per Al atom; (b) volume per formula unit; (c) intralayer cell parameter  $a$ ; (d) layer basal distance  $c'$ .

in samples with  $\text{M}^{\text{II}}$  and  $\text{M}^{\text{III}}$  cations of similar radius and ratio  $R \sim 2$ .<sup>18</sup> Vertical ordering has an effect on the energetics of the material, too, but whereas our results indicate that a hexagonal stacking is favored, experiments find that stackings with a high degree of disorder are preferred.<sup>18,20</sup> This discrepancy can be probably explained in terms of the small calculated energy differences between the samples, and the entropic effect on the thermodynamics of the systems at finite temperature.

As for the anions, we find that the Cl atoms preferentially occupy sites in the interlayer region that are vertically aligned with the trivalent cations.

**B. Dependence on Ratio  $R$ .** To study how the energetics and the structural parameters of hydrotalcite depend on  $R$ , two different series of calculations have been performed, one with a brucite-like 1H stacking (BC–BC–...) and another with a manasseite-like 2H stacking (BC–CB–BC–...). In all calculations, the trivalent cations have been distributed so as to maximize their distances, in accordance with the findings of subsection IVA. The results are summarized in Figure 2, and Table 2 provides detailed parameters for the investigated configurations.

Figure 2a shows the formation heat  $\Omega$  (per Al atom) as a function of  $R$ . This is calculated as

$$\Omega/N = (E_{\text{tot}} - E_{\text{brucite}})/N + (\mu_{\text{Mg}} - \mu_{\text{Al}} - \mu_{\text{Cl}}) \quad (2)$$

where  $\mu_X$  is the chemical potential for atom  $X$  in the gas phase. We can see that the dependence of  $\Omega$  on  $R$  is strongly nonlinear, with a minimum (implying greater stability) at  $R = 3$  for both stacking orders. It is also interesting to notice that the 2H stacking is energetically favored, i.e., is more stable, up to  $R = 4.33$ , where the 1H and 2H stackings become energetically equivalent. Higher  $R$  values correspond to samples more similar to brucite, and these results suggest that the brucite-like 1H stacking becomes increasingly favored in energy. On the other

**TABLE 2: Geometrical Parameters for [Mg,Al][Cl]-HTlc, with 1H and 2H Stackings, at Different  $R^a$** 

stacking	$R$	$\Omega$ ( $\text{\AA}^3$ )	$a$ , ( $\text{\AA}$ )	$c'$ ( $\text{\AA}$ )	MgO ( $\text{\AA}$ )	AlO ( $\text{\AA}$ )	layer thickness ( $\text{\AA}$ )
1H	1.67	36.85	3.012	7.023	2.056	1.915	1.973
1H	2.2	37.79	3.016	7.189	2.058	1.899	1.978–2.018
1H	3	38.20	3.026	7.219	2.058	1.904	1.981
1H	4.33	38.03	3.040	7.122	2.061	1.904	2.009–2.061
1H	$\infty$	25.03	3.110	4.476	2.067		2.043
2H	1.67	37.57	3.006	7.195	2.057	1.908	1.979
2H	2.2	37.80	3.017	7.185	2.058	1.908	1.977–2.019
2H	3	38.07	3.026	7.193	2.058	1.905	2.017
2H	4.33	36.40	3.036	6.833	2.061	1.905	2.004–2.057
2H	$\infty$	25.06	3.091	4.542	2.067		2.044

<sup>a</sup> Two values of the layer thickness are provided when the two layers in the simulation cell are not equivalent (odd number of Al atoms).

side, for  $R < 2$ , the presence of adjacent Al octahedra leads to increased electrostatic repulsions, and thus to a larger formation heat  $\Omega$ .

The dependences of the intralayer cell parameter  $a$  and basal spacing  $c'$  on  $R$  are shown in Figure 2c,d, respectively. The intralayer geometry is weakly affected by the chemical composition. A higher number of Al atoms slightly reduces  $a$ , as a consequence of the smaller atomic radius of Al ( $r_{\text{Al}} = 0.50 \text{ \AA}$ ) with respect to Mg ( $r_{\text{Mg}} = 0.65 \text{ \AA}$ ), and the behavior is almost linear in both series. This correlation has been reported in various experimental works.<sup>17,18,20</sup>

In contrast,  $c'$  shows a strongly nonmonotonic dependence on  $R$  with a maximum at  $R = 3$ , and this nonlinearity affects also the volume of the unit cell, as shown in Figure 2b. The decrease in  $c'$  and in volume at large  $R$  is not experimentally observed. This discrepancy may be related to the smallness of our simulation cell, which does not allow us to well describe diluted Al configurations. Moreover, in the experimental samples the presence of water molecules prevents any collapse of the interlayer distance.

On the other side, a small value of  $R$  corresponds to a higher electrostatic polarization of both intra- and interlayer regions: the stronger interactions reduce the distance between the layers, at the expense of the potential energy. This behavior has been both reported and predicted.<sup>17,18</sup> However, comparison of our results with experiment<sup>4,18,20,37</sup> is not immediate because the available data refer to systems where interlayer water molecules and different anions are usually present. The calculated  $c'$  is typically underestimated with respect to the experiment because of the reduced size of the interlayer region. At the same time, the layer octahedra in our simulations are less compressed along the vertical than in real samples, leading to a slight overestimation of the layer thickness (defined as the distance between the two planes where intralayer oxygens are situated) and an underestimation of  $a$ .

The results in Figure 2 suggest a direct connection between the behavior of the total energy and the volume of the samples. The most energetically favored configuration corresponds also to that of maximum volume. As previously noticed, in the limit  $R \rightarrow \infty$ , a brucite-like stacking becomes energetically favored, with simultaneously a smaller  $c'$  and volume. The smaller volume at low  $R$  for the brucite-like stacking could be an effect of stronger polarization and better packing of more highly concentrated anions and hydroxyl groups, which in this case are not facing each other across the interlayer space but are rotated  $60^\circ$  around a vertical axis passing through the anion. In the pure-Mg sample the 2H stacking is actually found to be unstable: our calculations show that upon relaxation one layer

**TABLE 3: Calculated Volume and Cell Parameters for HTlcs of Different Composition**

composition	$\Omega$ ( $\text{\AA}^3$ )	$a$ ( $\text{\AA}$ )	$c'$ ( $\text{\AA}$ )
[Mg,Al]·Cl	38.07	3.026	7.193
[Mg,Al]·OH	35.66	3.071	6.547
[Mg,Ga]·OH	36.49	3.111	6.532

shifts with respect to the other, so that the cations are not vertically aligned anymore.

## V. Results: Comparing HTlcs with Different $M^{\text{III}}$ Cations and Counterions

**A. Structural Properties.** To analyze the influence of the chemical species in HTlcs, we have compared the properties of [Mg,Al][Cl], [Mg,Al][OH], and [Mg,Ga][OH], while the ratio  $R$  ( $=3$ ) and, consequently, the number of anions were kept constant. The natural form of [Mg,Al]·OH is called meixnerite and is isomorphous with hydrocalcite. We chose the configuration that we found to be the most stable in the previous section, i.e., a 2H stacking with  $R = 3$ .

The structural parameters of the three HTlcs are reported in Table 3. We observe that the introduction of  $\text{OH}^-$  anions yields a large shrinking of the  $c'$  parameter, and a slight increase of the intralayer parameter  $a$ . The first effect can be attributed to both the smaller size of the hydroxyl anion with respect to  $\text{Cl}^-$  and the stronger interactions between the anions and the layers. A similar effect on  $a$  can be seen by substituting Al with larger Ga atoms: the intralayer parameter increases, and the interlayer parameter  $c'$  does not change remarkably.

Interestingly, the preferred sites for the  $\text{OH}^-$  anions are different from those for  $\text{Cl}^-$ : whereas in the latter case the anions are vertically aligned with the trivalent cations, the O atom of the hydroxyl anion lies at the center of a square formed by two pairs of H atoms facing each other across the interlayer region.  $\text{OH}^-$  is orthogonal to this square, and oriented along one of the hexagonally symmetrical directions of the brucite-like layer. The different configuration for  $\text{Cl}^-$  and  $\text{OH}^-$  suggests that also the interaction between the layers and the anions is different. In the case of  $\text{Cl}^-$ , electrostatic interactions dominate, as indicated by the fact that their preferential site is found to correspond to the minimum of the electrostatic potential of the HTlc layers, calculated in the absence of counterbalancing anions. For the hydroxyl anions, instead, the 4-fold coordination of their preferential binding site suggests an interaction with the layer OH groups stronger than the underlying electrostatic potential of the layers. These considerations are consistent with the shorter distance between the layers, and may provide an explanation for the increase of the intralayer parameter in the presence of hydroxyl anions in terms of the deformation due to the stronger interaction between layers and compensating anions.

**B. Electronic Properties.** The study of the electronic properties is an indispensable step for the understanding of the chemical behavior of the HTlcs. Several experiments have reported the large difference of activity of [OH]- and [Cl]-HTlcs for base-catalyzed reactions. In particular, this difference has been observed in the catalytic conversion of 2-methyl-3-butyn-2-ol (MBOH).<sup>38</sup> This substrate is indeed sensitive to the acid or basic character of the solid surface, and its conversion has been proposed<sup>39</sup> as a test reaction to determine the nature of the active sites. Noteworthy, when the samples are in the hydrated state, i.e., with a high amount of interlayer water, [OH]-HTlc is by far the most reactive for the base-catalyzed reaction. This behavior is consistent with the high reactivity (similar to NaOH) of the meixnerite-like [Mg,Al][OH]-HTlc, able to

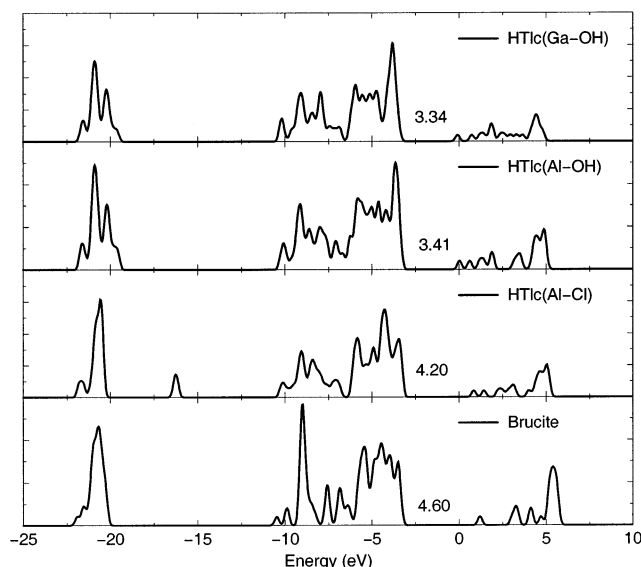


**Figure 3.** Electronic density of states of HTlcs and brucite. The centers of mass of the lowest bands have been aligned. The gap width is indicated in electronvolts.

perform, in liquid phase and at low temperature, the self-condensation of acetone,<sup>40</sup> the condensation of benzaldehyde and acetone<sup>41</sup> or that of citral and acetone.<sup>42</sup> In contrast to [OH]-HTlc, [Cl]-HTlc is poorly active for the catalytic conversion of MBOH.<sup>38</sup> Interestingly, for our study, this lower activity also prevails when both samples are compared in the dehydrated form; therefore when anionic species only are present in the interlayer space, which corresponds exactly to our model.

A first theoretical analysis can be done by comparing the electronic densities of states (EDOS) in the various cases studied. These densities are obtained by considering the valence electrons with the addition of the unoccupied conduction states. Figure 3 shows the EDOS of the investigated samples, together with that of brucite (to be used as a reference). To align the energy bands, we assumed that the centers of mass of the innermost bands (which can be attributed to O(2s) atomic states) are unaffected by chemical and geometric differences in the samples and are thus coincident. We can see that the introduction of trivalent cations and anions in the HTlcs reduces the gap between valence and conduction states with respect to brucite. In particular, the OH<sup>-</sup> anions reduce the gap by a much larger amount than Cl<sup>-</sup>, whereas no major difference occurs between samples with Ga or Al atoms. In addition, Figure 3 suggests that the shrinking of the gap is caused mostly by the decrease in energy of the LUMOs (lowest unoccupied molecular orbitals) rather than a higher energy of the HOMOs (highest occupied molecular orbitals). This feature, however, is determined by our somewhat arbitrary choice of the alignment of the bands and should thus be considered cautiously. If, for instance, the chemical potentials (~midgap energies) were aligned, the gap shrinkage would be more evenly distributed between increased HOMO and decreased LUMO energies.

Because the cation type, Al or Ga, does not make any substantial difference, in contrast with the anion Cl<sup>-</sup> or OH<sup>-</sup>, we examined the spatial densities of the near-gap states for [Mg,-Ga][OH]- and [Mg,Al][Cl]-HTlcs, to highlight their differences. We found that whereas the HOMOs are mainly intralayer O(2p) states, the LUMOs have more variable spatial distributions, mostly confined in the interlayer region, and not directly centered on the anions. By comparing the LUMOs of [Mg,Al][Cl]- and [Mg,Ga][OH]-HTlcs (see Figures 4-5), we can remark

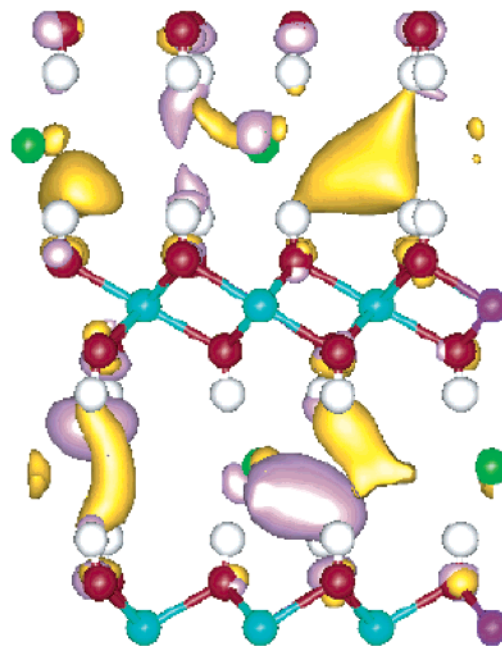


**Figure 4.** Spatial distribution of the two lowest conduction states for [Mg,Al][Cl]-HTlc. LUMO and LUMO+1 are indicated respectively by a yellow and lilac surface. Mg, Al, Cl, O, and H atoms are respectively turquoise, violet, green, red, and white.

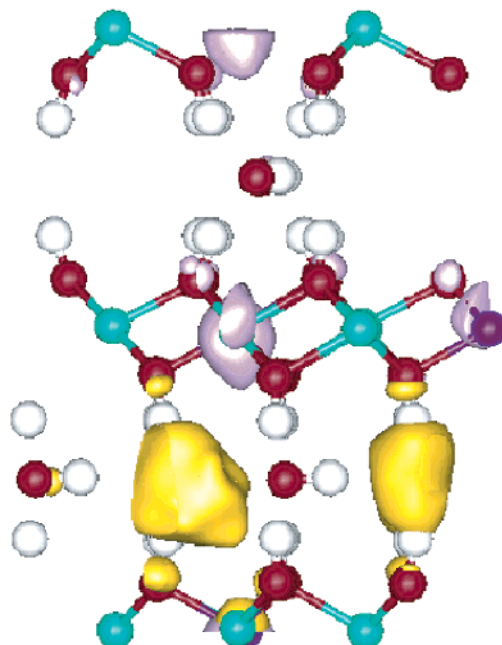
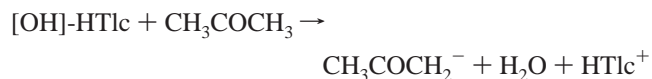


**Figure 5.** Spatial distribution of the two lowest conduction states for [Mg,Ga][OH]-HTlc. LUMO and LUMO+1 are indicated respectively by a yellow and lilac surface. Mg, Ga, O, and H atoms are respectively turquoise, violet, red, and white.

that, for the former, the empty states are quite dispersed throughout the interlayer region, whereas for the latter there are well-defined regions of localization in the interlayer region.

Experimentally, the larger basicity of [OH]-HTlcs with respect to [Cl]-HTlcs should govern the first step of the aldol formation. For example, in the case of acetone:



The interaction of [OH]-HTlc with acetone leads to the

intermediate species



which defines the activation energy needed to deprotonate acetone. There is no doubt that the  $\text{CH}_3\text{COCH}_2^-$  anion formation and, subsequently, the aldolization, depend on the barrier height to the proton abstraction. Relating experimental and theoretical information, we can understand that the reactive site involved in the deprotonation of acetone is more efficient in [OH]-HTlcs than in [Cl]-HTlcs. Indeed, the smaller band gap in [OH]-HTlcs, as well as the character of the LUMO, mainly localized between the two layers OH groups and the interstitial  $\text{OH}^-$  anions, represent favorable factors for the stabilization of the precursor species to  $\text{CH}_3\text{COCH}_2^-$  and thus lead to a decreased activation energy for acetone deprotonation.

As the density of states of [Cl]-HTLC and [OH]-HTLC do not show important differences between the HOMO energies, a similar basicity should be expected on the basis of Koopmans' definition (i.e., the higher the HOMO, the larger the aptitude to give electron density). However, relying on the much larger "basic" behavior of [OH]-HTLC reacting with acetone, one can argue that the supermolecular system formed by the hydrotalcite and the reactant has to be considered to explain the reactivity. Because the larger difference between [Cl]-HTLC and [OH]-HTLC is in their band gaps, one can propose that the larger activity of [OH]-HTLC is mainly related to a better stabilization of the anionic intermediate of the reaction, yielding a larger rate of the final product.

## VI. Summary and Conclusions

In this paper we have presented a theoretical study of anhydrous hydrotalcite-like compounds based on first principles periodic density functional calculations with a variable simulation cell. This approach has allowed us to fully optimize in a very efficient way the complex structures of these compounds, by simultaneously relaxing both the lattice parameters and the internal degrees of freedom. In turn, this has allowed us to study a large number of different systems, and thus establish a correlation between structural parameters, formation energies and chemical composition. For instance, our results show the existence of a minimum of the formation energy as a function of the  $\text{M}^{\text{II}}/\text{M}^{\text{III}}$  ratio  $R$  at  $R \sim 3$ , in good agreement with experimental stability ranges for these materials. At the same time a nonmonotonic behavior of the interlayer distance, with a maximum at the same value  $R \sim 3$ , is found, suggesting a connection between energetic stability and structure.

Another important goal of this work has been to provide some rationalization of the observed differences in the activity as basic catalysts of hydrotalcites containing different types of cations and interlayer anions. In particular, we have tried to understand the reasons of the larger basicity of  $[\text{Mg,Ga}][\text{OH}]\text{-HTlcs}$  with respect to  $[\text{Mg,Al}][\text{Cl}]\text{-HTlcs}$ . As a first step in this direction, we have studied the energies and character of the electronic states of these compounds and found that it is the nature of the anions to have a major influence on the electronic properties. Moreover, we have found that in [OH]-HTlcs the HOMO–LUMO energy gap is smaller and the LUMO is spatially more localized in the interlayer region. This leads to a larger electron acceptor character in this region, which can explain why the basic site in [OH]-HTlcs is more active than that in [Cl]-HTlcs.

**Acknowledgment.** We are grateful to A. Pasquarello, S. Scandolo, and P. Giannozzi for useful discussions. The calcula-

tions of this work have been performed at the Swiss Center for Scientific Computing, in Manno.

## References and Notes

- (1) Trifirò, F.; Vaccari, A. In *Comprehensive Supramolecular Chemistry*; Atwood, J. L., Davies, J. E. D., MacNicol, D. D., Vögtle, F., Eds.; Pergamon Press: Oxford, U.K., 1996; Vol. 7, pp 251–91.
- (2) Cavani, F.; Trifirò, F.; Vaccari, A. *Catal. Today* **1991**, *11*, 173.
- (3) Vaccari, A. *Catal. Today* **1998**, *41*, 53.
- (4) Aramendía, M. A.; Avilés, Y.; Benítez, J. A.; Borau, V.; Jiménez, C. V.; Marinas, J. M.; Ruiz, J. R.; Urbano, F. J. *Micropor. Mesopor. Mater.* **1999**, *29*, 319.
- (5) Prinetto, F.; Tichit, D.; Tessier, R.; Coq, B. *Catal. Today* **2000**, *55*, 103.
- (6) Tichit, D.; Naciri Bennani, M.; Figueras, F.; Ruiz, J. R. *Langmuir* **1998**, *14*, 2086.
- (7) Prinetto, F.; Ghiotti, G.; Durand, R.; Tichit, D. *J. Phys. Chem. B* **2000**, *104*, 11117.
- (8) Car, R.; Parrinello, M. *Phys. Rev. Lett.* **1985**, *55*, 2471.
- (9) Car, R.; Parrinello, M. In *Simple Molecular Systems at Very High Density*; Polian, A., Loubeyre, P., Boccaro, N., Eds.; Plenum Press: New York, 1989; p 455.
- (10) Raugei, S.; Silvestrelli, P. L.; Parrinello, M. *Phys. Rev. Lett.* **1999**, *83*, 2222.
- (11) Parrinello, M.; Rahman, A. *Phys. Rev. Lett.* **1980**, *45*, 1196.
- (12) Focher, P.; Chiarotti, G. L.; Bernasconi, M.; Tosatti, M.; Parrinello, M. *Europhys. Lett.* **1994**, *36*, 345.
- (13) Bernasconi, M.; Chiarotti, G. L.; Focher, P.; Scandolo, S.; Tosatti, E.; Parrinello, M. *J. Phys. Chem. Solids* **1994**, *56*, 501.
- (14) Allmann, R. *Am. Miner.* **1968**, *53*, 1057.
- (15) Allmann, R. *Acta Crystallogr. B* **1968**, *24*, 972.
- (16) Arakcheeva, A. B.; Pushcharovskij, D. Y.; Rastsvetaeva, R. K.; Atensio, D.; Lubman, G. Y. *Kristallografiya* **1996**, *41*, 1024.
- (17) López-Salinas, E.; García-Sánchez, M.; Montoya, J. A.; Acosta, D. R.; Abasolo, J. A.; Schifter, I. *Langmuir* **1997**, *13*, 4748.
- (18) Bellotto, M.; Rebours, B.; Clause, O.; Lynch, J.; Bazin, D.; Elkaïm, E. *J. Phys. Chem.* **1996**, *100*, 8527.
- (19) Brindley, G. W.; Kikkawa, S. *Am. Miner.* **1979**, *64*, 836.
- (20) Pausch, I.; Lohse, H.-H.; Schürmann, K.; Allmann, R. *Clays Clay Mater.* **1986**, *34*, 507.
- (21) Schaper, H.; Berg-Slot, J. J.; Stork, W. H. *J. Appl. Catal.* **1989**, *54*, 79.
- (22) López-Salinas, E.; García-Sánchez, M.; Ramón-García, M. L.; Schifter, I. *J. Porous Mater.* **1996**, *3*, 169.
- (23) Mascolo, G.; Marino, O. *Mineral. Mag.* **1980**, *43*, 619.
- (24) Allmann, R. *Chimia* **1970**, *24*, 99.
- (25) De Roy, A.; Forano, C.; El Malki, K.; Besse, J. P. In *Expanded Clays and Other Microporous Materials*; Occelli, M. L., Robson, H. E., Eds.; Reinhold: New York, 1992; Vol. 2, pp 108–69.
- (26) Galli, G.; Pasquarello, A. In *Computer Simulations in Chemical Physics*; Allen, M. P., Tildesley, D. J., Eds.; Kluwer Academic Publisher: The Netherlands, 1993; pp 261–313.
- (27) Kohn, W.; Vashista, P. In *Theory of the Inhomogeneous Electron Gas*; Lundqvist, S., March, N. H., Eds.; Plenum Press: New York, 1983; p 79.
- (28) Andersen, H. C. *J. Chem. Phys.* **1980**, *72*, 2384.
- (29) Ancilotto, F.; Chiarotti, G. L.; Scandolo, S.; Tosatti, E. *Science* **1997**, *275*, 1288. Serra, S.; Cavazzoni, C.; Chiarotti, G. L.; Scandolo, S.; Tosatti, E. *Science* **1999**, *284*, 788. Laio, A.; Bernard, S.; Chiarotti, G. L.; Scandolo, S.; Tosatti, E. *Science* **2000**, *287*, 1027.
- (30) Vanderbilt, D. *Phys. Rev. B* **1990**, *41*, 7892.
- (31) Laasonen, K.; Pasquarello, A.; Car, R.; Lee, C.; Vanderbilt, D. *Phys. Rev. B* **1993**, *47*, 10142.
- (32) Bachelet, G. B.; Hamann, D. R.; Schlüter, M. *Phys. Rev. B* **1982**, *26*, 4199.
- (33) Perdew, J. P.; Chevary, J. A.; Vosko, S. H.; Jackson, K. A.; Pederson, M. R.; Singh, D. J.; Fiolhais, C. *Phys. Rev. B* **1992**, *46*, 6671.
- (34) Zigan, F.; Rothbauer, R. *Neues. Jahr. Mineral. Monat.* **1967**, 137.
- (35) Perdew, J. C.; Zunger, A. *Phys. Rev. B* **1981**, *23*, 5048.
- (36) Radoslovich, E. W. *Am. Miner.* **1963**, *48*, 76.
- (37) Xu, Z. P.; Zeng, H. C. *J. Phys. Chem. B* **2001**, *105*, 1743.
- (38) Constantino, V. R. L.; Pinnavaia, T. J. *Inorg. Chem.* **1995**, *34*, 883.
- (39) Lauron-Pernot, H.; Luck, F.; Popa, J. M. *Appl. Catal.* **1991**, *78*, 213.
- (40) Tichit, D.; Naciri Bennani, M.; Figueras, F.; Tessier, R.; Kervennal, J. *Appl. Clay Sci.* **1998**, *13*, 401.
- (41) Rao, K. K.; Gravelle, M.; Valente, J.; Figueras, F. *J. Catal.* **1998**, *173*, 115.
- (42) Roelofs, J. C. A. A.; van Dillen, A. J.; de Jong, K. P. *Catal. Today* **2000**, *60*, 297.